MONTE-CARLO-BASED TRAINING AND APPLICATION FRAMEWORK FOR ENHANCED NONLINEAR AERODYNAMIC REDUCED-ORDER MODELING

M. Winter, C. Breitsamter
Technical University of Munich
Department of Mechanical Engineering
Chair of Aerodynamics and Fluid Mechanics
Boltzmannstr. 15, 85748 Garching, Germany

Abstract

In the present work, a Monte-Carlo-based aerodynamic reduced-order modeling process is developed to estimate statistical errors caused by the random training data segmentation. The reduced-order models (ROMs) considered here are constructed by means of a linear or nonlinear system identification. Therefore, training, validation, and test datasets provided by a computational fluid dynamics (CFD) solver are exploited. However, system identification tasks always involve parameter optimization and function fitting problems that are sensitive to the choice of the initial parameters or the training data composition, respectively. Consequently, an unfavorable random starting point may lead to a poor ROM performance. A remedy to overcome those model uncertainties is the application of a Monte-Carlo training and application strategy. To assess the effectiveness of the proposed ROM framework, the procedure is demonstrated by modeling the unsteady transonic aerodynamics of the pitching and plunging NLR 7301 airfoil. Various ROM techniques are trained and applied within the Monte-Carlo framework to show their simulation capabilities compared to the respective full-order CFD solution. The focus is particularly laid on the evaluation of the ROM solution's fluctuation due to different random initializations. It is shown that some ROM approaches exhibit a very good agreement combined with a low sensitivity to the training data partitioning, which is highly beneficial for a reliable and accurate application.

1 INTRODUCTION

In order to increase the efficiency and safety of future aircraft within the scope of the set emission and fuel consumption targets (ACARE 2050), it is necessary to understand and efficiently predict the static and dynamic interactions between the elastic, aerodynamic, and inertial forces. The well-developed potential flow methods used so far for the unsteady aerodynamic modeling, however, cannot fully meet today's accuracy requirements, especially, when the focus is on the transonic flow regime. In contrast, the air loads can be determined with sufficient accuracy using modern CFD approaches. However, the extensive use of CFD requires very high computational capacities, which severely limits their application for aeroelastic purposes. A promising way to save computational resources is the development and application of reduced-order models that are calibrated by means of CFD-based data. In the course of this investigation, CFD-generated training data representing the dominant input/output relations of the considered system are utilized in terms of a linear or nonlinear identification. Once the ROMs are available, the models can be used to provide accurate and reliable aerodynamic responses, without the need to perform further time-consuming CFD calculations. In the following, selected identification-based ROM approaches are briefly recapitulated.

An overview of aerodynamic ROMs such as Volterra-theory-based methods [1, 2] or the POD [3, 4] is given by Dowell and Hall [5] as well as Lucia et al. [6]. Moreover,

approaches developed within the system identification and control community have been utilized for unsteady aerodynamic reduced-order modeling, e.g., the eigensystem realization algorithm (ERA) [7–10], the auto-regressive with exogenous input (ARX) model [11], and the auto-regressive moving average (ARMA) model [12]. Considering linear systems only, the ERA, ARX, and ARMA identification techniques are suited to obtain a ROM of the underlying unsteady aerodynamics. However, the prediction of large amplitude motions or nonlinear parameter influences such as varying freestream conditions requires nonlinear system identification approaches in order to capture the inherent nonlinearities. Thus, the use of multilayer-perceptron (MLP) neural networks has been proposed by Faller and Schreck [13], Voitcu and Wong [14] as well as Mannarino and Mantegazza [15]. ROM approaches based on Kriging interpolation were investigated by Glaz at al. [16] and Liu et al. [17]. Furthermore, radial basis function (RBF) neural networks have been successfully applied by Zhang et al. [18], Lindhorst et al. [19] and Winter and Breitsamter [20]. Recently, very promising results for nonlinear unsteady aerodynamic reduced-order modeling have been achieved by by Kou et al. [21,22] and Winter and Breitsamter [10, 23].

Nonetheless, nonlinear identification techniques are always sensitive to the choice and composition of the training data or the selection of the initial parameters [24]. Commonly, the available dataset characterizing the system to be investigated is partitioned, while about 70% of the randomly chosen samples are used for the parameter estimation (training); see Nelles [24] or Winter and Breitsamter [23] for instance. In contrast, the remaining samples are used for validation and test purposes. Hence, the ROMs as well as the results generated by them are subject to uncertainties induced by the random data composition. As a consequence, it is unclear whether the ROM output is a coincidence/outlier or if the ROM results are reproducible with high probability. Two scenarios can be considered exemplarily: On the one hand, a good model performance might be ascertained for a specific ROM, whereas models trained by other data compositions or initial settings yield a comparatively poor agreement with the reference/test data. On the other hand, it is possible that a given ROM performs not satisfactory, although all representative and necessary information about the underlying system are available within the training dataset. Both cases should be avoided since they cover the true potential of the identification approach.

To address the aforementioned issues, a Monte-Carlo-based training and application framework for unsteady aerodynamic reduced-order modeling is suggested in this work, which is independent from the employed identification algorithm. By estimating statistical errors due to the model construction process, it can be ensured that the ROM results become both reproducible and comparable. This also leads to an increased transparency between the solutions obtained by different identification-driven ROM techniques. For demonstration purposes, the Monte-Carlo procedure is used to model the unsteady transonic aerodynamics of the pitching and plunging NLR 7301 airfoil. In this regard, selected ROMs, namely the ARX [11], MLP [15], LOLIMOT [23], and LOLIMOT-MLP [10] approaches, are constructed and applied within the proposed Monte-Carlo framework to show their simulation capabilities. For all cases, the respective full-order CFD solution serves as the reference. It is shown that some ROM approaches produce severe simulation output variations caused solely by the random data segmentation. In contrast, there are also ROM methods that seem less sensitive to those initialization uncertainties. Hence, the importance of the present research in terms of selecting and comparing various aerodynamic ROM algorithms is outlined.

2 Monte-Carlo Framework for Aerodynamic Reduced-Order Modeling

In order to make the previously motivated model uncertainties measurable, a Monte-Carlo-based training and application strategy is employed. In general, Monte-Carlo approaches are characterized by repeated numerical simulations that are initialized by random processes [25]. Here, N_{MC} independent ROMs are trained in parallel as can be seen in Fig. 1, whereas all model and identification parameters are kept constant. Due to the random data segmentation process, which is performed autonomously for each of the N_{MC} models, the finally obtained ROMs are different from each other. Consequently, they won't produce the same response for a given user-defined input sig-

nal. However, it is important to emphasize that the CFD-based dataset containing the training, validation, and test data is the same for all ROMs. As the CFD simulation yielding the training data is the main computational cost driver for system-identification-based unsteady aerodynamic reduced-order modeling, the additional effort of the suggested Monte-Carlo procedure can be justified.

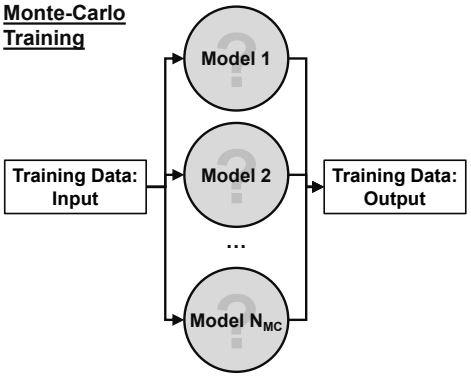

Figure 1: Monte-Carlo training procedure for system-identification-based aerodynamic reduced-order modeling.

After the N_{MC} ROMs have been trained, they can be utilized for the intended application purposes. According to Fig. 2, the same user-defined input signals are fed into each ROM resulting in N_{MC} different output time series. Given those ROM responses, statistical methods can be applied to analyze the data. In the present work, the mean of the response (μ_i) as well as the standard deviation (σ_i) is evaluated for comparison and classification purposes. Defining $y_{i,j}(k)$ as the ith model output element at time step k produced by ROM j, the following equations are evaluated:

$$\mu_i(k) = \frac{1}{N_{MC}} \sum_{j=1}^{N_{MC}} y_{i,j}(k) \tag{1}$$

$$\sigma_i(k) = \sqrt{\frac{1}{N_{MC}-1} \sum_{j=1}^{N_{MC}} \left(y_{i,j}(k) - \mu_i(k) \right)^2} \tag{2}$$

3 Results

For demonstration of the Monte-Carlo methodology, the aerodynamic characteristics of the NLR 7301 airfoil are studied.

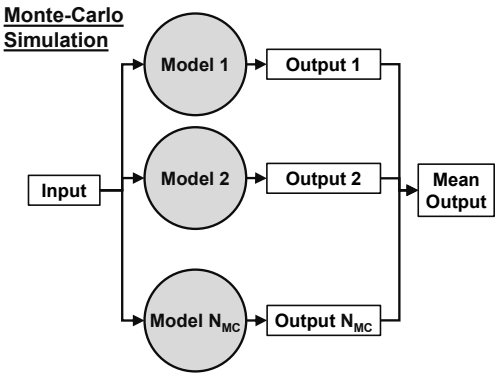

Figure 2: Application procedure using the previously generated N_{MC} ROMs.

3.1 Test Case

The supercritical NLR 7301 airfoil undergoing a pitching and plunging motion is a well-known test case in the unsteady aerodynamic and aeroelastic community [26, 27]. As it can be seen in Fig. 3, the flow at a freestream Mach number of $Ma_\infty = 0.753$ and an angle of attack of $\alpha = 0.6^\circ$ is dominated by a strong shock located on the airfoil's suction side. For sufficiently large excitation amplitudes, the variation of both the shock intensity and the shock position becomes non-linearly related to the displacement. Hence, also the forces and moments are influenced in a nonlinear way. For the sake of simplicity, viscous effects are excluded from these considerations by solving the Euler equations using the in-house CFD code AER-Eu [28, 29]. As the focus in this work is laid on an intermethod comparison, the Euler-based modeling does not restrict the validity of these studies.

The geometrical properties of the NLR 7301 airfoil can be described by a chord length of $c_{ref} = 0.3\ m$, while the pitching axis is located at 40% of the chord according to Zwaan [26]. The structured multi-block grid used for the CFD simulations (see also Fig. 3) contains 14,396 volume cells [10].

3.2 Training Methodology

For the unsteady forced-motion CFD computations, a constant freestream Mach number of $Ma_\infty = 0.753$ and an angle of attack of $\alpha = 0.6^\circ$ have been defined corresponding to Fig. 3. Moreover, rigid body deflections are enforced in order to investigate the motion-induced aerodynamics of the NLR 7301 airfoil. The resulting air load response is

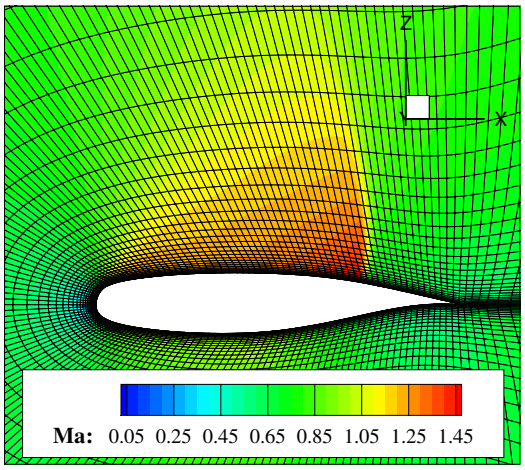

Figure 3: Computational grid of the NLR 7301 airfoil along with the computed steady-state Mach number contours at $Ma_\infty = 0.753$ and $\alpha = 0.6^\circ$ (AER-Eu).

computed by means of the AER-Eu solver. Here, the respective lift and pitching moment coefficient time series $C_L(\tau)$ and $C_{M_y}(\tau)$ are the CFD outputs of interest, while the reference point for the pitching moment is defined as the quarter-chord point. Thus, the system inputs are considered with the pitching angle $\theta(\tau)$ and the plunging degree of freedom $h(\tau)$, whereas the system outputs are $C_L(\tau)$ and $C_{M_y}(\tau)$. According to Fig. 4, a total excitation range of $-5.5^\circ < \theta < 5.5^\circ$ and $-11\%\ c_{ref} < h < 11\%\ c_{ref}$ is chosen for the training signals. As a consequence of the conducted time step convergence study, the excitation signals are resolved with a nondimensional time step size of $\Delta\tau = 0.01$. However, for the ROM training datasets a time discretization of $\Delta\tau = 0.1$ is sufficient. Hence, the data used for ROM identification consists of 8200 samples; see Fig. 4. Resulting from a single CFD run, the unsteady aerodynamic response caused by the forced pitching and plunging motions is obtained. The AER-Eu output time series in terms of C_L and C_{M_y} is depicted in Fig. 5. It should be emphasized that the information contained in Figs. 4 and 5 represents the full dataset from which all identification-based models are derived in the following. In order to highlight the advantages of the Monte-Carlo simulation framework discussed in Sec. 2, four different ROM methods have been trained exploiting the available data:

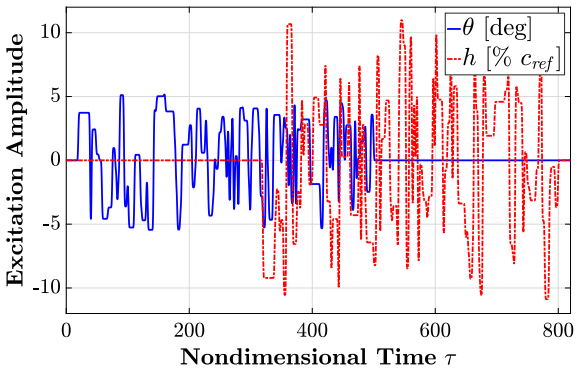

Figure 4: Training signals for the forced-motion excitation of the pitch and plunge degrees of freedom ($\Delta\tau = 0.1$).

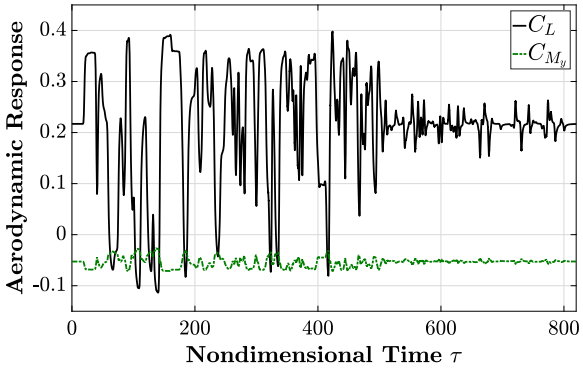

Figure 5: Lift and pitching moment coefficient response caused by the user-defined excitation (NLR 7301, $Ma_\infty = 0.753$, $\alpha = 0.6^\circ$, $\Delta\tau = 0.1$, AER-Eu).

1) ROM/ARX [11]
2) ROM/LOLIMOT [23]
3) ROM/MLP [15, 24]
4) ROM/LOLIMOT-MLP [10]

As detailed information about the identification procedures, the user-defined settings, and the modus operandi of the ROMs are out of the scope of this paper, the reader is referred to the work of Winter and Breitsamter [10] for a thorough discussion.

For each of the four ROM approaches listed above, $N_{MC} = 10$ models have been constructed according to the schematic presented in Fig. 1. As a result, 40 different models are available for simulating the aerodynamic system. However, since the models were trained by the same dataset, the computationally most expensive step of the ROM generation, namely the CFD computation, had to be performed only once. As it will be shown in the following, the additional insights arising from the Monte-Carlo methodology justify the marginally increased computational effort.

3.3 Application and Discussion

In the following, the reduced-order models are utilized for generically designed application tests. In this way, the Monte-Carlo application procedure in combination with a statistical analysis of the ROM responses is outlined.

In Fig. 6, the filtered white Gaussian noise (FWGN) signals, which have been defined for testing purposes, are shown. Using the a priori trained ROMs, the aerodynamic response caused by the FWGN signal excitation can be efficiently computed. However, in order to assess the quality of the ROM results, a reference AER-Eu computation has been carried out as well. The lift coefficient resulting from this consideration is presented in Fig. 7.

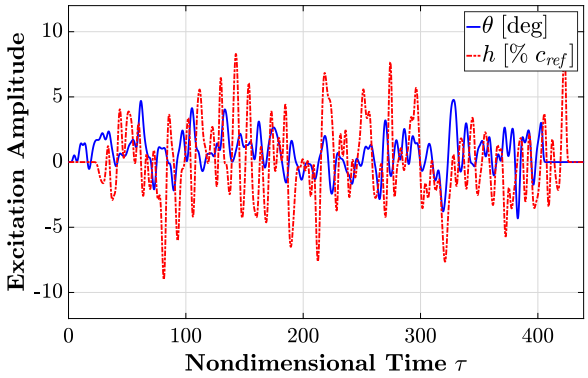

Figure 6: Generic FWGN signals for the simultaneous excitation of the pitch and plunge degrees of freedom. Amplitude range: $-5° < \theta < 5°$, $-10\%\ c_{ref} < h < 10\%\ c_{ref}$.

Based on the Monte-Carlo framework, the mean and the standard deviation of the ROM outputs can be calculated for the $N_{MC} = 10$ models. In the following, the mean μ for a particular ROM type is visualized by the main line. In contrast, the standard deviation σ is shown by a transparent shade.

Supported by Fig. 8 displaying the pitching moment coefficient, the following conclusions about the ROM output's mean and standard deviation can be drawn: For comparatively small standard deviations there is a high probability that also individual models produce approximately the mean response. Besides, a small σ can indicate that representative and well-resolved training data had been available in the associated amplitude and frequency regime. However, small standard deviations are not a guarantee for a high accuracy of the ROM result. In contrast, large standard deviations can indicate a lack of training data or a possible unstable simulation behavior. Consequently, high standard deviations are usually linked to model outputs of poor quality.

Furthermore, the statistical information can be exploited to obtain further insights regarding the strengths and weaknesses of different ROM approaches. It can be asserted that the linear ROM/ARX model captures the trend of the response quite well. However, the linear model is not flexible enough to reproduce the correct amplitude levels. This is an indicator that the system is governed by pronounced nonlinearities. In contrast, the ROM/MLP approach performs much better than the previously considered linear model. Though, the MLP neural network employed in recurrent operation frequently encounters simulation instabilities. This behavior can be seen by means of the locally increased standard deviation in Fig. 8. Although the large fluctuations of the MLP solution are restricted to a certain

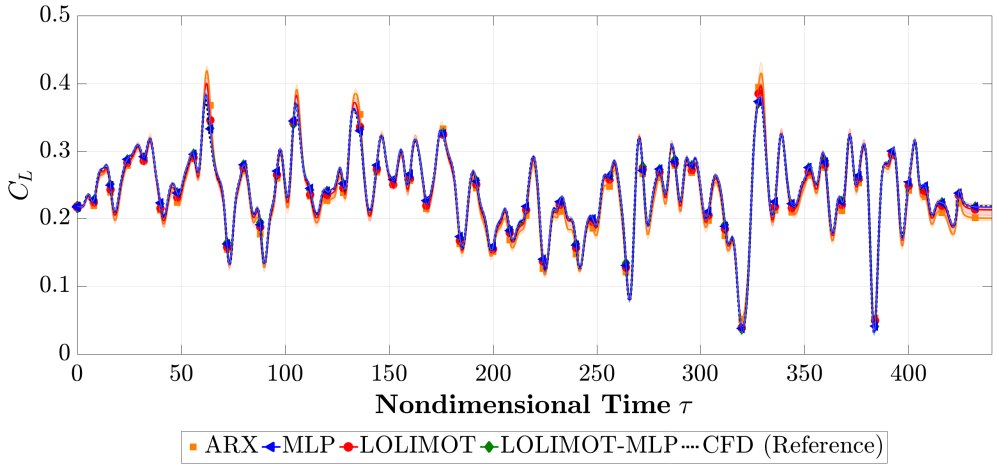

Figure 7: Lift coefficient response due to the FWGN excitation depicted in Fig. 6 (NLR 7301, $Ma_\infty = 0.753$, $\alpha = 0.6°$).

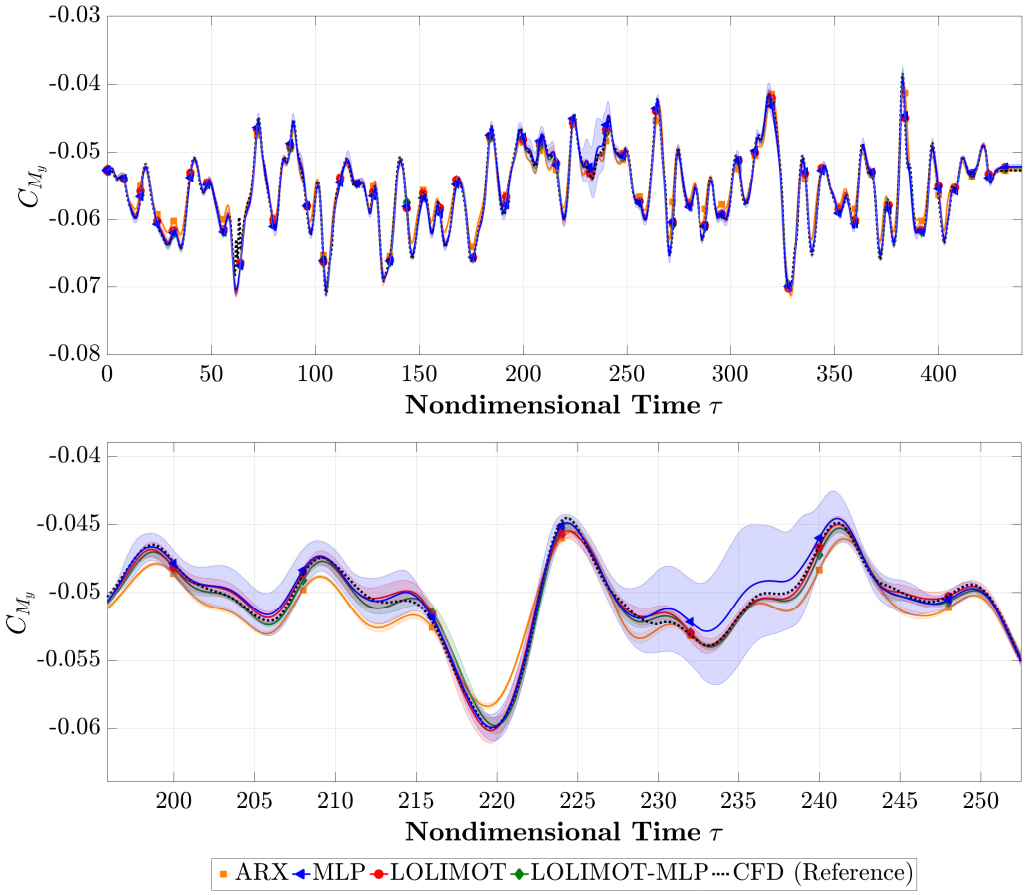

Figure 8: Top: Pitching moment coefficient induced by the FWGN excitation shown in Fig. 6 (NLR 7301, $Ma_\infty = 0.753$, $\alpha = 0.6°$). Bottom: Detail cutout from the diagram depicted on top.

region in the present case, they can become globally dominant and, consequently, corrupt the ROM results. Both the ROM/LOLIMOT and ROM/LOLIMOT-MLP approaches accurately reproduce the CFD reference, while the influences of the random training data composition on the solution are comparatively small. The LOLIMOT-MLP method yields the best agreement, which can be underpinned by the very low standard deviations.

Finally, the ROMs are tested using an amplitude-scaled variant of the previously considered FWGN signals; see Fig. 9. Hence, the excitation amplitudes have been limited to the range $-0.1° < \theta < 0.1°$ and $-0.5\%\ c_{ref} < h < 0.5\%\ c_{ref}$. As it has been shown in [10], the application of ROMs trained with large amplitude motions towards small amplitude cases is a challenging task. Based on the graphs for C_L depicted in Fig. 10, it can be seen that the ARX model exhibits the largest discrepancies compared to the CFD reference. A distinct offset can be detected for the linear model along with drastically increased values for

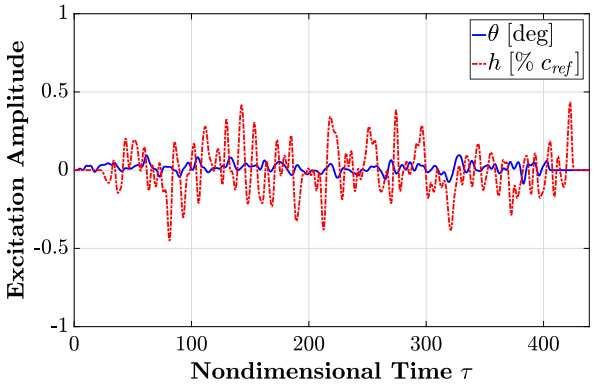

Figure 9: Generic FWGN signals for the simultaneous excitation of the pitch and plunge degrees of freedom. Amplitude range: $-0.1° < \theta < 0.1°$, $-0.5\%\ c_{ref} < h < 0.5\%\ c_{ref}$.

the standard deviation. Also the outputs of the independently trained $N_{MC} = 10$ LOLIMOT models (see the bottom of Fig. 10) deviate from each other. Thus, the models strongly depend on the random training data initialization. At this point it is worth to indicate a very helpful

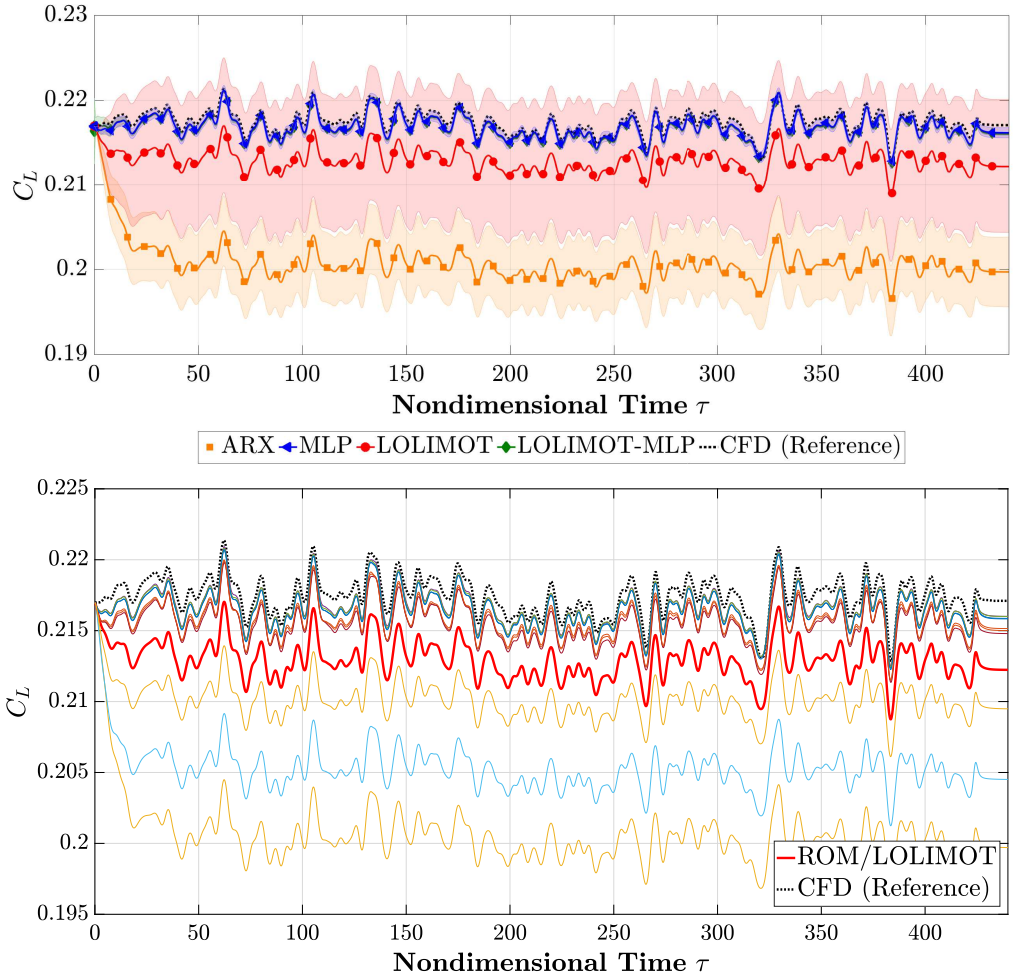

Figure 10: Top: Lift coefficient response due to the FWGN excitation depicted in Fig. 9 (NLR 7301, $Ma_\infty = 0.753$, $\alpha = 0.6^\circ$). Bottom: Visualization of the ROM/LOLIMOT responses for all $N_{MC} = 10$ cases along with the mean ROM output and the CFD reference.

feature of the Monte-Carlo strategy: Without the knowledge about the CFD reference, the user becomes able to judge about the possible accuracy of the ROM solution by considering the standard deviation. Both the ROM/ARX and the ROM/LOLIMOT solutions seem to be unreliable as they are characterized by large σ values. This can be confirmed by a comparison between the mean response and the additionally computed reference result. In contrast, ROM/MLP and ROM/LOLIMOT-MLP match the CFD-generated curve with good accuracy, while also exhibiting comparatively small standard deviations of the model responses.

Last but not least, the comparability and reproducibility of different ROM results is enhanced via the Monte-Carlo strategy since outliers and poor performing individual models can be identified.

4 Conclusions

In this paper, a Monte-Carlo-based framework for unsteady aerodynamic reduced-order modeling was presented in theory and application. It was demonstrated that in many cases the ROM approaches produce pronounced simulation output variations that are caused for example by the random training data partitioning. The suggested training and application strategy combined with a statistical post-processing can be utilized to quantify and assess the solution quality of identification-based ROMs. In this way, the Monte-Carlo approach leads to an increased knowledge concerning the reliability and robustness of the trained models. Moreover, if several ROM approaches are available, a decision about the most appropriate model can be made based on the statistical information. Finally, the com-

parability and reproducibility of results generated by aerodynamic reduced-order models can be enhanced.

REFERENCES

[1] Silva, W. A., *Discrete-Time Linear and Nonlinear Aerodynamic Impulse Responses for Efficient CFD Analyses: Ph.D. Dissertation*, College of William and Mary, Williamsburg, VA, 1997.

[2] Raveh, D. E., "Reduced-Order Models for Nonlinear Unsteady Aerodynamics," *AIAA Journal*, Vol. 39, No. 8, 2001, pp. 1417–1429.

[3] Hall, K. C., Thomas, J. P., and Dowell, E. H., "Proper Orthogonal Decomposition Technique for Transonic Unsteady Aerodynamic Flows," *AIAA Journal*, Vol. 38, No. 10, 2000, pp. 1853–1862.

[4] Iuliano, E. and Quagliarella, D., "Proper orthogonal decomposition, surrogate modelling and evolutionary optimization in aerodynamic design," *Computers & Fluids*, Vol. 84, 2013, pp. 327–350.

[5] Dowell, E. H. and Hall, K. C., "Modeling of Fluid-Structure Interaction," *Annual Review of Fluid Mechanics*, Vol. 33, No. 1, 2001, pp. 445–490.

[6] Lucia, D. J., Beran, P. S., and Silva, W. A., "Reduced-Order Modeling: New Approaches for Computational Physics," *Progress in Aerospace Sciences*, Vol. 40, No. 1-2, 2004, pp. 51–117.

[7] Silva, W. A. and Bartels, R. E., "Development of Reduced-Order Models for Aeroelastic Analysis and Flutter Prediction Using the CFL3Dv6.0 Code," *Journal of Fluids and Structures*, Vol. 19, No. 6, 2004, pp. 729–745.

[8] Silva, W. A., "Simultaneous Excitation of Multiple-Input/Multiple-Output CFD-Based Unsteady Aerodynamic Systems," *Journal of Aircraft*, Vol. 45, No. 4, 2008, pp. 1267–1274.

[9] Fleischer, D. and Breitsamter, C., "Efficient Computation of Unsteady Aerodynamic Loads Using Computational-Fluid-Dynamics Linearized Methods," *Journal of Aircraft*, Vol. 50, No. 2, 2013, pp. 425–440.

[10] Winter, M. and Breitsamter, C., "Nonlinear Identification via Connected Recurrent and Static Neural Networks," *Nonlinear Dynamics (Under Review)*, 2017.

[11] Zhang, W. and Ye, Z., "Reduced-Order-Model-Based Flutter Analysis at High Angle of Attack," *Journal of Aircraft*, Vol. 44, No. 6, 2007, pp. 2086–2089.

[12] Raveh, D. E., "Identification of Computational-Fluid-Dynamics Based Unsteady Aerodynamic Models for Aeroelastic Analysis," *Journal of Aircraft*, Vol. 41, No. 3, 2004, pp. 620–632.

[13] Faller, W. E. and Schreck, S. J., "Unsteady Fluid Mechanics Applications of Neural Networks," *Journal of Aircraft*, Vol. 34, No. 1, 1997, pp. 48–55.

[14] Voitcu, O. and Wong, Y. S., "Neural Network Approach for Nonlinear Aeroelastic Analysis," *Journal of Guidance, Control, and Dynamics*, Vol. 26, No. 1, 2003, pp. 99–105.

[15] Mannarino, A. and Mantegazza, P., "Nonlinear Aeroelastic Reduced Order Modeling by Recurrent Neural Networks," *Journal of Fluids and Structures*, Vol. 48, 2014, pp. 103–121.

[16] Glaz, B., Liu, L., and Friedmann, P. P., "Unsteady Aerodynamic Modeling Using a Surrogate-Based Recurrence Framework," *AIAA Journal*, Vol. 48, No. 10, 2010, pp. 2418–2429.

[17] Liu, H., Hu, H., Zhao, Y., and Huang, R., "Efficient Reduced-Order Modeling of Unsteady Aerodynamics Robust to Flight Parameter Variations," *Aerospace Science and Technology*, Vol. 49, 2014, pp. 728–741.

[18] Zhang, W., Wang, B., Ye, Z., and Quan, J., "Efficient Method for Limit Cycle Flutter Analysis Based on Nonlinear Aerodynamic Reduced-Order Models," *AIAA Journal*, Vol. 50, No. 5, 2012, pp. 1019–1028.

[19] Lindhorst, K., Haupt, M., and Horst, P., "Efficient surrogate modelling of nonlinear aerodynamics in aerostructural coupling schemes," *AIAA Journal*, Vol. 52, No. 9, 2014, pp. 1952–1966.

[20] Winter, M. and Breitsamter, C., "Reduced-Order Modeling of Unsteady Aerodynamic Loads Using Radial Basis Function Neural Networks," *63rd Deutscher Luft- und Raumfahrtkongress, Augsburg,*

Germany, Deutsche Gesellschaft für Luft- und Raumfahrt Paper 2014-340013, 2014, pp. 1–10.

[21] Kou, J., Zhang, W., and Yin, M., "Novel Wiener Models with a Time-Delayed Nonlinear Block and their Identification," *Nonlinear Dynamics*, Vol. 85, No. 4, 2016, pp. 2389–2405.

[22] Kou, J. and Zhang, W., "Layered Reduced-Order Models for Nonlinear Aerodynamics and Aeroelasticity," *Journal of Fluids and Structures*, Vol. 68, 2017, pp. 174–193.

[23] Winter, M. and Breitsamter, C., "Neurofuzzy-Model-Based Unsteady Aerodynamic Computations Across Varying Freestream Conditions," *AIAA Journal*, Vol. 54, No. 9, 2016, pp. 2705–2720.

[24] Nelles, O., *Nonlinear System Identification: From Classical Approaches to Neural Networks and Fuzzy Models*, Springer-Verlag, Berlin, Germany, 2001.

[25] McCracken, D. D., "The Monte Carlo Method," *Scientific American*, Vol. 192, No. 5, 1955, pp. 90–96.

[26] Zwaan, R. J., "Summary of Data Required for the AGARD SMP Activity 'Standard Aeroelastic Configurations' – Two-Dimensional Configurations," *NLR, MP 79015 U*, 1979.

[27] Dietz, G., Schewe, G., and Mai, H., "Experiments on Heave/Pitch Limit-Cycle Oscillations of a Supercritical Airfoil Close to the Transonic Dip," *Journal of Fluids and Structures*, Vol. 19, No. 1, 2004, pp. 1–16.

[28] Kreiselmaier, E. and Laschka, B., "Small Disturbance Euler Equations: Efficient and Accurate Tool for Unsteady Load Prediction," *Journal of Aircraft*, Vol. 37, No. 5, 2000, pp. 770–778.

[29] Pechloff, A. and Laschka, B., "Small Disturbance Navier-Stokes Method: Efficient Tool for Predicting Unsteady Air Loads," *Journal of Aircraft*, Vol. 43, No. 1, 2006, pp. 17–29.